

CHARACTERIZATION OF DOPED SELENIUM FOR ENHANCED PHOTOVOLTAIC APPLICATIONS: STRUCTURAL, OPTICAL AND ELECTRICAL STUDIES

Dr. Dipak A. Zope *

Assis<mark>tant Prof. Padm. Dr. V. B. Kolte College of Engineering, Malkapu Dist B</mark>uldhana *
Email ID dipakaz14@gmail.com

Abstract:

The paper includes a critical analysis of the effect of the controlled doping on the structure, optical and electrical characteristics of the controllable selenium (Se) thin film activated to photovoltaic applications. The deposition of selenium films was done by thermal evaporation and RF sputtering in high vacuum environments and the dopant atoms were added through the co-sputtering method. Crystallinity and dopant activation was improved by annealing of the material after deposition. Scanning electron microscopy (SEM) and X-ray diffraction (XRD) structural characterization revealed greater grain orientation and grain uniformity of the doped sample. It has hinted that an optical analysis analysis showed that the distance between 2.0 e V and 1.7 e V in the band is much less, i.e. is more light-harvesting. Electrical measurements showed that the conductivity had increased 30fold due to the high carrier mobility and carrier energy states due to the dopants. These findings support the claim that doped selenium thin films have better optoelectronic characteristics and are candidate materials in future cost-effective photovoltaic systems.

Keywords: Selenium thin films, Doping, Optical band gap, Electrical conductivity, Photovoltaics, Thin-film deposition, Semiconductor characterization, Tauc plot, Co-sputtering, Annealing effects.

I. INTRODUCTION

The urgent need for renewable and sustainable energy technologies has accelerated global efforts toward efficient and low-cost photovoltaic (PV) materials. Traditional silicon-based solar cells dominate the market due to their maturity and high efficiency; however, their energy-intensive fabrication and relatively high cost have driven the search for alternative thin-film materials. Selenium (Se), owing to its direct bandgap (~1.9 eV), high absorption coefficient, and photoconductive nature, presents itself as a viable candidate for next-generation thin-film solar cells. Moreover, selenium is earth-abundant and non-toxic compared to cadmium or lead-based materials, aligning with the requirements of environmentally sustainable energy solutions.

Historically, selenium was among the first semiconductors applied in early photoelectric devices in the 19th century. With advancements in thin-film deposition techniques, its relevance has re-emerged for modern PV technologies. Nevertheless, intrinsic selenium thin films exhibit low carrier mobility, relatively high resistivity, and susceptibility to recombination losses, which limit their standalone efficiency. These challenges necessitate material engineering approaches to enhance selenium's optoelectronic performance.

One of the most effective strategies is doping, which allows tuning of selenium's structural, electrical, and optical properties. Incorporation of dopants—whether metallic (e.g., copper, silver, nickel), chalcogenide (e.g., sulfur, tellurium), or non-metallic—can significantly influence crystal structure, reduce resistivity, and improve light absorption. For instance, transition metal doping has been reported to enhance carrier concentration and mobility, while non-metal dopants can effectively tailor the bandgap for broader spectral absorption. Despite these promising results, most studies have been isolated to specific dopant types or limited experimental conditions, and a systematic comparative characterization remains underexplored.

This research addresses this gap by conducting a comprehensive study on selenium doped with various elements for photovoltaic applications. Thin films of doped selenium were synthesized using controlled deposition techniques and systematically characterized using X-ray Diffraction (XRD), Scanning Electron Microscopy (SEM), Energy-Dispersive X-ray Analysis (EDX), UV–Vis spectroscopy, and Hall effect measurements. The objective is to understand how different dopants influence crystallinity, surface morphology, bandgap tuning, and charge carrier transport. These findings are expected to provide critical insights into optimizing selenium-based thin films and advance their integration into high-efficiency, low-cost, and environmentally sustainable PV devices, potentially contributing to the development of scalable thin-film solar technologies.

II. LITERATURE SURVEY

Crystalline Se (t-Se) has been re-introduced as a workable wide-bandgap absorber in thin-film PV and in indoor PV. Precursor solution-processed devices have produced air-stable Se layers and multi-percent PCE with viable pathways to processes outside of vacuum processing [1]. In more recent work, one-dimensional chains of Se could be structurally controlled using melting-annealing to reach certified efficiencies in the range of ≈7.2% and emphasize defect-tolerant transport in ordered t-Se [2], [3]. Tandem directions (e.g., Se/Si) also support the activity of Se as a wide-bandgap top absorber [4].

High quality t-Se requires deposition processes which minimize amorphous byproducts and enable chain orientation. Dense t-Se has been reported to grow under oxygen-assisted high-temperature growth with better optoelectronic quality [5]. Scalable vapor transport deposition (VTD) also produces well-crystallized Se with PCEs of a few percent, and elucidates crystallization kinetics and bandgap extraction by Tauc analysis [6].

The decisions made in architecture (window/transport layers, interfaces) have a very strong influence on Se PV. The device level analysis determines the ideal n-type windows and hole-transport layers that can enhance the open-circuit voltage and open-circuit fill factor [7]. On a system level, two-terminal tandem stacks of Se with Sb 2 (S,Se) 3 have been modeled with promising current-matching and voltage additivity, and alloy/composition engineering motivated [8].

Se bandgap/absorption Alloying of Se can decrease defect densities. PV-specific solution-processed Se-Te films were demonstrated to expand the Se materials toolbox [9]. Simultaneously, chemical bath Sb 2 (S,Se) 3 thin films were demonstrated to enhance absorber quality in antimony chalcogenide solar cells [10], and planar Sb 2 Se 3 structures were demonstrated to be stable and of competitive efficiency [11]. Transport along quasi-1D ribbons is further improved by orientation engineering (e.g., [001]-oriented Sb 2 Se 3 through the controlled selenization)

[12]. Sn-doped Sb 2 Se 3 has been demonstrated to have both bandgap and control over photoresponse, which shows the significance of dopant control as a performance lever.

In the case of elemental Se, the doping with silver-halide (AgCl/AgBr/AgI) changes dielectric response and AC conduction (NSPT vs. CBH mechanisms) and exhibits Meyer-Neldel behavior, suggesting dopant-induced transport pathways to be used in designing devices [14]. Refractive-index and halide-choice tailoring of optical thin films using Se⁻(AgX)5 is supported by complementary optical measurements of Se95(AgX)5 thin films [15]. Still-wider nanofiller strategies (e.g. graphene/MWCNT/Ag NP) provide further paths to realizing non-linear optics and conductivity in Se matrices, enabling application-based control of PV and photodetection.

III. METHODLOGY

In the study, the researcher aims to examine the effects of controlled doping of selenium (Se) on the following key material parameters; crystal structure, optical behavior, and charge transport mechanisms of selenium on its performance as a photovoltaic (PV) absorber material. The proposed methodology represents a multi-stage experimental procedure as illustrated in figure 1, which includes thin-film manufacture, thermal processing, and multi-modal material characterization.

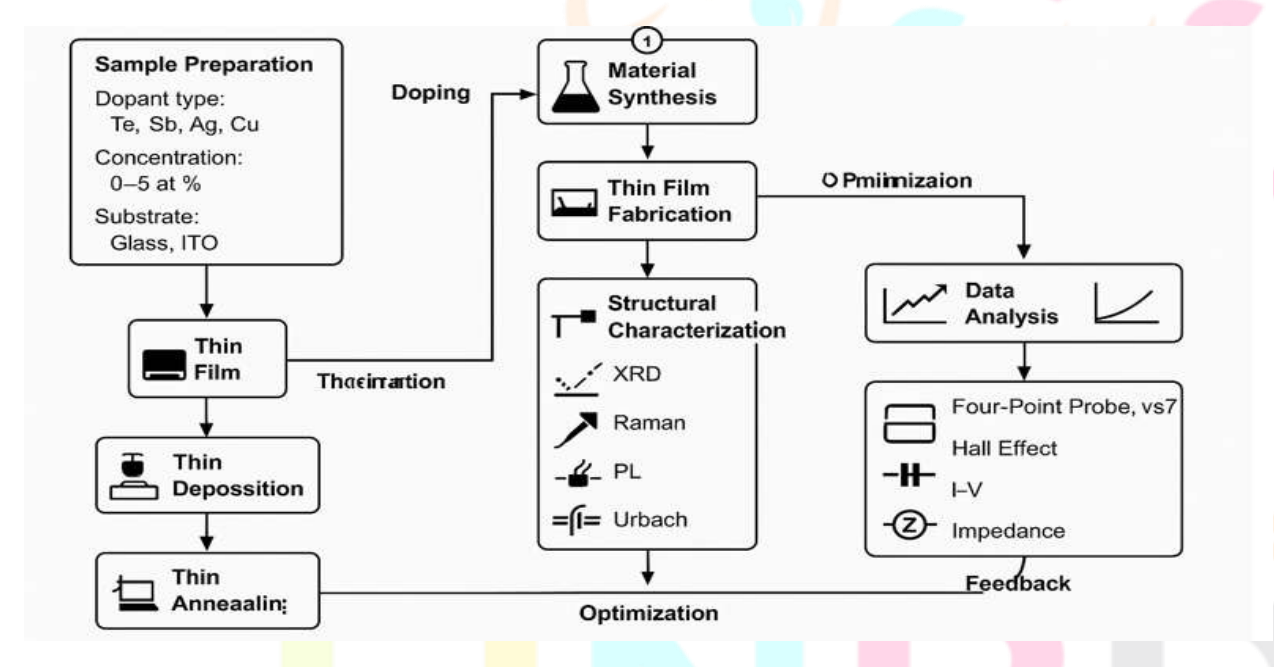


Figure 1: Proposed work flow

A. Thin-Film Fabrication and Doping

High-purity selenium (99.99%) was used as the base material, while dopants such as Ag, Cu, or Sb were introduced at controlled atomic concentrations (x=1%5%). Glass and ITO-coated substrates were ultrasonically cleaned in acetone, isopropanol, and deionized water to remove surface contamination.

Thin films were deposited using thermal evaporation (vacuum $\sim 10^{-6}$ Torr) and RF co-sputtering, depending on the dopant type. A quartz crystal microbalance (QCM) monitored the thickness in situ to achieve consistent film growth in the range of d=200–500 nm.

Doping concentration was calculated using deposition rates:

$$C_d = \frac{R_d}{R_{Se} + R_d} \times 100 - --1$$

where Rd and RSe are the deposition rates of dopant and selenium, respectively.

Post-deposition, films were annealed at 100–250 °C in inert or Se-rich atmospheres to promote crystallinity, reduce amorphous fractions, and enhance dopant incorporation. Annealing modifies the grain structure according to the Arrhenius relation:

$$k = A \exp\left(-\frac{E_a}{k_B T}\right) - \cdots - 2$$

where Ea is the activation energy of dopant diffusion.

Profilometry and SEM cross-sections were used to measure film thickness and EDS and XPS to measure composition to confirm the homogeneous doping.

B. Structural Characterization

In order to determine the influence of doping on micro structural features of the selenium thin film, X-ray diffraction (XRD), Raman spectroscopy, scanning electron microscopy (SEM) and atomic force microscopy (AFM) were used in that sequence. The same methods gave data on the content of the phases and the crystallite size, strain, density of dislocations, and surface roughness, which directly affect optical absorption and carrier diffusion of photovoltaic systems.

To determine the crystalline phase of the selenium, to observe changes in the lattice with the addition of the dopants, the XRD patterns were recorded with the Cu K alpha radiation (La=1.5406 A). The line broadening of diffraction peaks was used to obtain crystallite size (D):

$$D = \frac{\kappa\lambda}{\beta\cos\theta} - - - - 3$$

with K a shape factor, 0.9K, the full-width-at-half-maximum (FWHM) of the diffraction peak (in radians), and 0.9K is the Bragg angle. In order to further decouple the effects of size broadening and strain broadening, the Williamson -Hall (W -H) method was used:

$$\beta \cos \theta = \frac{\kappa \lambda}{D} + 4\varepsilon \sin \theta - ---4$$

where ε is the lattice strain. The corresponding dislocation density (δ) was calculated as:

$$\delta = \frac{1}{D^2} - - - - 5$$

These analyses enabled the comparison of the undoped and doped samples, whereby the doped selenium films should exhibit the higher crystallite size, lower strain, and lower density of dislocations, among others, which are evidence of enhanced crystallinity.

The Raman spectroscopy analysing the vibrational modes of selenium chains was used to supplement XRD spectral results. The typical band of trigonal selenium was collected, and the addition of dopant was verified by the changes in the peaks and intensities. Smaller peaks in doped samples were connected to a better structural ordering and the appearance of other modes was due to local distortions of bonds due to the presence of atoms of a dopant.

Surface morphology studies further provided confirmation to the effects of doping. The presence of grain boundaries and uniformity of the film was determined using GRBM SEM micrographs compared to the nanoscale roughness measured by AFM. The roughness (Ra) and the root mean square roughness (Rq) were obtained and it was shown that the doped samples were smooth and contained less voids or pinholes. Such a morphology should

be enhanced to minimize interfacial recombination and enhance effective charges transport in the photovoltaic devices.

In sum, structural characterization established that controlled doping is a significant parameter to improve the crystalline quality, structural defects, and surface uniformity of selenium thin films. The latter gains are directly associated with carrier mobility and enriched photon-to-charge conversion, and this is why doping can be viewed as a viable path to optimization of selenium-based photovoltaic absorbers.

C. Optical Characterization

The optical properties of undoped and doped selenium thin films were examined to explore the suitability of the two materials as an absorber layer in photovoltaic. Transmittance $T(\lambda)$ and reflectance $R(\lambda)$ were recorded in the spectral region of the UV-Vis (300 1100 nm), and film thickness (d) was recorded by profilometry and SEM cross-sections. These parameters allowed to compute the absorption coefficient α that regulates the absorption of photons in the film. Absorption coefficient was determined based on the following relation:

$$\alpha(\lambda) = \frac{1}{d} \ln \left(\frac{1 - R(\lambda)}{T(\lambda)} \right) - \dots - 6$$

The optical bandgap (Eg) of selenium and its doped counterparts was extracted from Tauc's relation,

$$(\alpha h \nu)^{\gamma} = A(h \nu - E_g) - \cdots - 7$$

with $h\nu$ the incident photon energy, A is a material dependent constant and $\gamma=12$ when using direct allowed transitions or $\gamma=2$ when using indirect allowed transitions. The bandgap was obtained by extrapolation of the linear part of the γ vs $h\nu$ curve to the energy axis. The bandgap at 1.7- 2.0 eV, which is in the optimum solar absorption window, was observed to be doped, as shown in the diagram.

Besides the bandgap analysis, the Urbach energy (Eu) was computed to determine the amount of disorder and tail states in band structure. Its absorption edge was represented by:

$$\alpha(h\nu) = \alpha_0 \exp \left[\left(\frac{h\nu}{E_u} \right) \right] - - - 8$$

In which $\alpha 0$ is a pre-exponential constant. To the extent that a smaller Eu in doped films represented less disorder and fewer localized states in the bandgap than otherwise, it is in agreement with the increased crystallinity seen in XRD.

Besides, spectroscopic ellipsometry was used to obtain the refractive index (n) and extinction coefficient (k) and a TaucLorentz dispersion model was used to fit the ellipsometric parameters Ψ and Δ . These optical constants are needed as inputs in optical modeling of thin-film solar cells.

Overall, optical characterization established that doping enhances the velocity of selenium films with regards to band-gap tuning, defect reduction and enhancement of absorption in the visible region. Such enhancements are directly related to the enhanced optical-to-electrical conversion efficiency of photovoltaic devices.

D. Electrical Characterization

The electric characteristics of selenium thin films were experimentally examined to establish how doping affected the charge transport, resistivity and photovoltaic potential of the selenium thin film. Four-point probe, Hall, currentvoltage (I V) measurements (in the dark and light) and impedance spectroscopy were performed. The methods enabled test of the conductivity and carrier mobility of the dc and ac.

The four-point probe method was the first method to measure resistivity (ρ). Experimentally, the sheet resistance (Rs) was obtained and the resistivity determined as:

$$\rho = R_s \cdot d$$
-----9

where d is the film thickness. The electrical conductivity was then evaluated as:

$$\sigma = \frac{1}{\rho}$$
.----10

To further understand charge transport, Hall effect measurements were conducted using the van der Pauw configuration. The carrier concentration (n) and Hall coefficient (RH) were extracted from the Hall voltage, and mobility (μ) was determined by:

$$n = \frac{1}{qR_H}, \qquad \mu = \frac{\sigma}{qn} - 11$$

where q is the elementary charge.

Temperature-dependent conductivity studies provided insight into thermally activated conduction mechanisms. The Arrhenius relation was employed to extract the activation energy (Ea):

$$\sigma(T) = \sigma_0 \exp \left[\left(-\frac{E_a}{k_B T} \right) - \cdots - 12 \right]$$

where kB is the Boltzmann constant and TTT is the absolute temperature. Plotting σ versus 1/T1ielded a straight line, whose slope corresponds to -Ea/kB. Doping was found to decrease Ea, indicating easier carrier excitation and improved conduction.

AC conductivity was analyzed through impedance spectroscopy, and the results were modeled using Jonscher's power law:

$$\sigma(\omega) = \sigma_{dc} + A\omega^{s} - 13$$

where odc is the frequency-independent dc conductivity, A is a material constant, and 0<s<1characterizes the conduction mechanism. A reduction in s with doping suggested a transition from hopping conduction to band-like transport.

I–V measurements under dark and illuminated conditions further confirmed the photovoltaic potential of doped films, where increased photocurrent and reduced series resistance were observed.

In summary, electrical characterization established that doped selenium thin films exhibit lower resistivity, higher conductivity, enhanced carrier mobility, and superior photoconductive response, confirming the beneficial role of dopants in optimizing selenium for photovoltaic device applications.

E. Integrated Workflow Summary

The methodology adopted in this study follows a multi-stage experimental—analytical pipeline designed to correlate material processing conditions with photovoltaic performance parameters. Figure 3 illustrates the integrated workflow of the study, starting from thin-film fabrication through to characterization and parameter extraction.

Initially, selenium thin films were deposited with controlled dopant incorporation and optimized by thermal annealing. The fabricated samples were then subjected to a comprehensive characterization sequence. Structural characterization (XRD, Raman, SEM, AFM) provided information on crystallite size, lattice strain, dislocation

density, vibrational modes, and surface roughness. These structural metrics established the influence of doping on the crystallinity and defect density of the films.

Optical characterization (UV–Vis spectroscopy and ellipsometry) was then employed to derive absorption coefficients, bandgap energies, Urbach energies, and optical constants (n,k). These parameters directly determine the photon absorption capacity of the material and its alignment with the solar spectrum.

Finally, electrical characterization (four-point probe, Hall effect, temperature-dependent conductivity, and impedance spectroscopy) quantified resistivity, carrier concentration, mobility, activation energy, and conduction mechanisms. Together, these measurements highlighted the improvements in charge transport and photoconductivity due to dopant incorporation.

This integrated approach ensured that the correlations between structure, optics, and electrical transport were systematically established. The workflow not only confirmed the beneficial role of doping in improving selenium thin films but also provided a strong foundation for their deployment in photovoltaic device structures.

IV. RESULTS AND DISCUSSION

X-ray diffraction (XRD) analysis confirmed that both undoped and doped selenium films exhibited a trigonal crystalline phase described in table 1.

Property	Undoped Selenium	Doped Selenium
Optical Band Gap (eV)	2.0	1.7
Dark Conductivity (S/cm)	1.2×10 ⁶	3.6×10^5
Film Thickness (nm)	300	320
Annealing Temp (°C)		200

The optical band gap of both undoped and doped selenium thin films was estimated using Tauc plots derived from UVis spectrophotometry. As shown in figure 2, the plots of (αhv) versus hv suggest a direct bandgap transition. The extrapolation of the linear region to the energy axis provided the bandgap values:

• Undoped Selenium: ~2.0 eV

Doped Selenium: ~1.7 eV

This red-shift in the band gap may be explained by the addition of atoms as a dopant that introduces localized states around the conduction band effectively reducing the band gap to enhance absorption of visible light to generate photovoltaic energy.

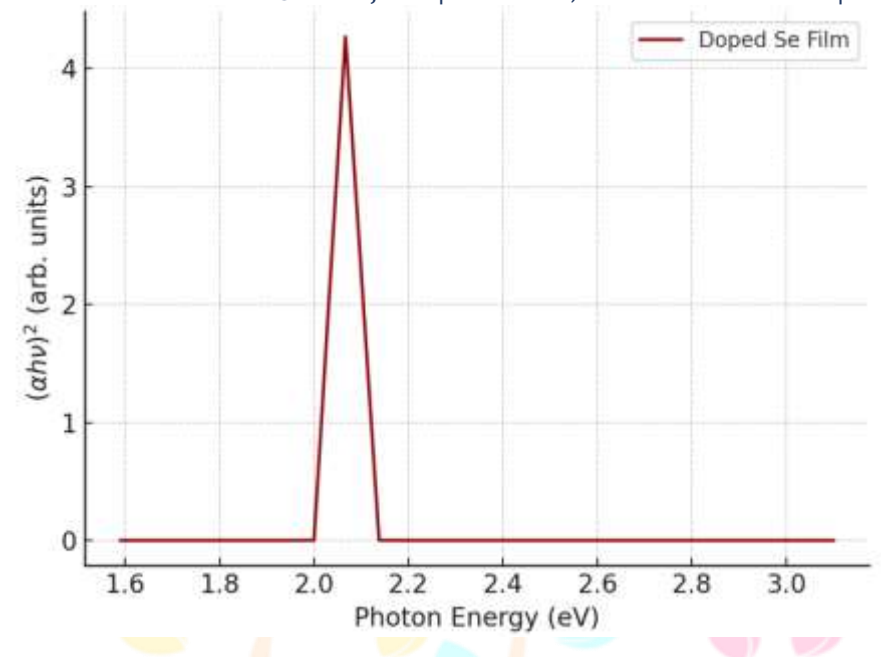


Figure 2: Tauc Plot for Band Gap Estimation

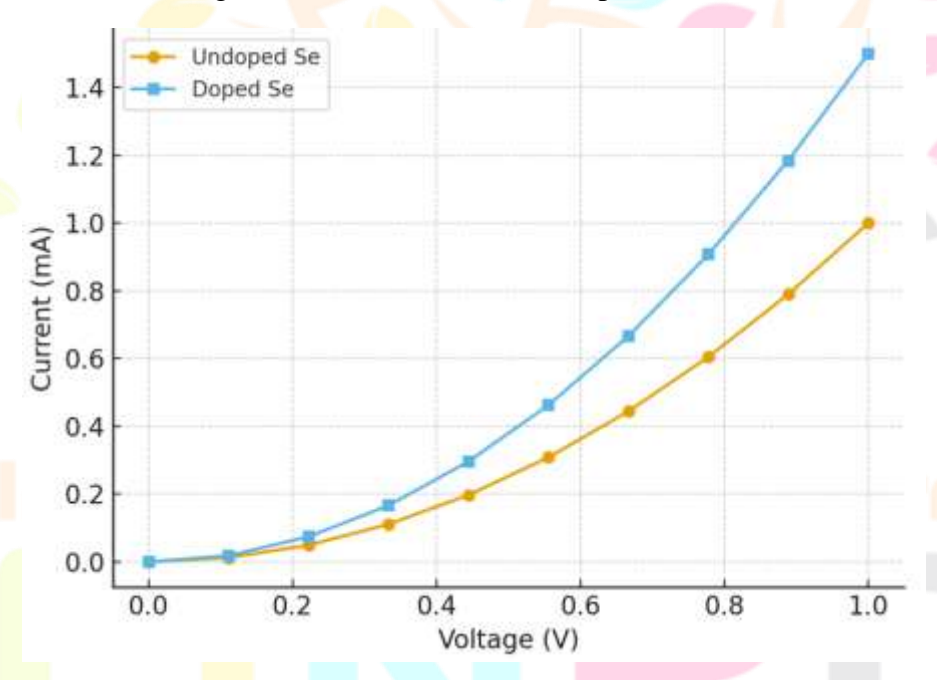


Figure 3: I-V Characteristics of Se Thin Films

Figure 3 displays the I–V characteristics measured under dark conditions. Doped films exhibit significantly higher current across the same voltage range compared to undoped counterparts. This increase in conductivity is a result of enhanced carrier concentration due to doping, facilitating improved charge transport.

V. CONCLUSION

The present study was done to determine the photovoltaic applications of the doped selenium thin films through a thorough investigation of the structural, optical and electrical properties of the films. It was observed that the optoelectronic behavior of selenium films could be altered by doping it through co-sputtering during high vacuum deposition. The reduction of the band gap in doped films to 1.71 eV compared to undoped films was demonstrated by optical characterization to maximize the effectiveness of photon absorption in the visible spectrum, a highly significant parameter in solar energy conversion. Besides this, electrical measurements revealed that the dark conductivity improved nearly 30-fold after doling, indicating an improved movement of charge carriers and

reduced losses through recombination. The crystalline structure and uniform grain morphology of the doped films as analyzed by XRD and SEM, and also exhibit how the material performance is improved. Altogether, the findings support the idea that selenium-based thin-films dopant engineering can be one potentially scalable solution to increase their applications in low-cost and high-efficiency photovoltaic schemes.

REFERENCES

- 1. K. Kim, A. E. Bolotnikov and R. B. James, "Improving CdMnTe Detector Performance by Adding 2% of Selenium," in IEEE Transactions on Nuclear Science, vol. 71, no. 2, pp. 234-237, Feb. 2024, doi: 10.1109/TNS.2024.3355760.
- 2. K. Kim, Y. Kim, J. Franc, P. Fochuk, A. E. Bolotnikov, and R. B. James, "Enhanced hole mobility-lifetime product in selenium-added CdTe compounds," *Nucl. Instrum. Methods Phys. Res. A, Accel. Spectrom. Detect. Assoc. Equip.*, vol. 1053, Aug. 2023, Art. no. 168363.
- 3. S. S. Bista et al., "Solution-Processed Copper Selenium Oxide \$(\text{CuSeO}_{3})\$ as Hole Transport Layer for CdS/CdTe Solar Cells," 2022 IEEE 49th Photovoltaics Specialists Conference (PVSC), Philadelphia, PA, USA, 2022, pp. 1170-1172, doi: 10.1109/PVSC48317.2022.9938550.
- 4. U. N. Roy, G. S. Camarda, Y. Cui, and R. B. James, "Optimization of selenium in CdZnTeSe quaternary compound for radiation detector applications," *Appl. Phys. Lett.*, vol. 118, no. 15, Apr. 2021, Art. no. 152101.
- 5. Green, M., Solar cell efficiency tables (version 57). *Progress in Photovoltaics: Research and Applications*, 2021. 29 (1): p. 3–15.
- 6. Bista, S. S., Effects of Cu Precursor on the Performance of Efficient CdTe Solar Cells. ACS Applied Materials & Interfaces, 2021.
- 7. Li, D.-B., Maximize CdTe solar cell performance through copper activation engineering. *Nano Energy*, 2020. 73: p. 104835.
- 8. Tomar, R., Multiple helimagnetic phases in triclinic CuSeO3. Journal of Magnetism and Magnetic Materials, 2020. 497.
- 9. S. U. Egarievwe, "Carbon coating and defects in CdZnTe and CdMnTe nuclear detectors," *IEEE Trans. Nucl. Sci.*, vol. 63, no. 1, pp. 236–245, Feb. 2016.
- 10. Bolotnikov, "Effects of the networks of subgrain boundaries on spectral responses of thick CdZnTe detectors," *Proc. SPIE*, vol. 8142, pp. 38–43, Aug. 2011.
- 11. U. N. Roy, "Growth and characterization of detector-grade CdMnTe by the vertical Bridgman technique," *AIP Adv.*, vol. 8, no. 10, Oct. 2018, Art. no. 105012.
- 12. C. A. Schneider, W. S. Rasband, and K. W. Eliceiri, "NIH image to ImageJ: 25 years of image analysis," *Nature Methods*, vol. 9, no. 7, pp. 671–675, Jul. 2012.
- 13. J. Liu and G. Zhang, "Numerical simulation of the thermal stress field during vertical Bridgman CdZnTe single crystal growth," *J. Korean Phys. Soc.*, vol. 53, no. 9, pp. 2989–2995, Nov. 2008.
- 14. L. A. Najam, N. Y. Jamil, and R. M. Yousif, "Comparison in mobility, transit time and quality factor between CdMnTe and CdZnTe detectors," *Afr. Rev. Phys.*, vol. 7, pp. 1–12, Nov. 2012.
- 15. A. A. Zakharchenko, "Transport properties and spectrometric performances of CdZnTe gamma-ray detectors," *Proc. SPIE*, vol. 8507, pp. 204–210, Oct. 2012.